
**HEAT AND MASS TRANSFER
AND PHYSICAL GASDYNAMICS**

Numerical Simulation of Swirling Flows in Vortex Tubes

O. V. Kazantseva, Sh. A. Piralishvili, and A. A. Fuzeeva

Rybinsk State Academy of Aviation Engineering, Rybinsk, Yaroslavl oblast, Russia

Received April 2, 2004

Abstract—Complete Navier–Stokes equations are solved numerically for the case of an intense swirling flow in an axisymmetric channel with an orifice plate in the delivery cross section and a throttle in the form of a peripheral slit at the opposite end. Flow patterns and velocity and temperature fields are obtained. The presence of precession of axial vortex is observed, as well as the formation of large-scale vortex structures. The numerical calculation results are compared for the first time with the experimental data obtained using Ranque–Hilsch energy separators.

INTRODUCTION

Because of a combination of special features of flow, which make it possible to intensify the processes of heat and mass transfer and provide for temperature stratification (Ranque effect) and cleaning and drying of gases, as well as for their separation, swirling flows attract ever closer attention of scientists in various countries. This attention is due both to the interest associated with the tendency for their more extensive application and to the necessity of theoretical interpretation of all effects observed experimentally in such flows.

It is known that local swirling of flow is widely employed in energy-related facilities and other technical devices for the organization and intensification of flow and heat transfer. Experimental investigations reveal that intense swirling of flow has a marked impact on the redistribution of total enthalpy, results in improvement of the process of preparation of mixtures as a result of intensification of mass transfer, and causes an increase in the intensity of combustion in reacting flows and in the capacity of a jet for aerodynamic stabilization of flame in combustors of aircraft engines.

The development and commercialization of new technologies and equipment calls for studies of the local, integral, and turbulent properties of swirling flow in various (often quite specific) devices such as, for example, channels with a longitudinally varying flow area, channels with an orifice plate in the outlet cross section, and so on.

Although extensive experimental data are presently available on the gas dynamics of swirling flows, no consensus of opinion exists on the mechanism of energy separation and temperature stratification in such flows. The hypothesis of vortex interaction suggested by A.P. Merkulov and developed further by his disciples [1] is taken to be the most validated one. This hypothesis was later used by Frohlingsdorf and Unger [2] for numerical simulation of the process of energy separation in the Ranque–Hilsch vortex tube. They calculated compressible flow and simulated the effect of temperature separation in a vortex tube. The flow was described by the conservation equations for mass, momentum, and energy. The Keyes correction [3] was used to calculate turbulent viscosity, and the thus obtained value of the coefficient of turbulent viscosity was taken to be constant over the entire grid. The time step was 0.4×10^{-3} to 0.8×10^{-3} s. Frohlingsdorf and Unger [2] gave profiles of the tangential component of velocity, which made it possible to compare the numerical calculation results with experimental data. Comparison of the structures of axial and peripheral flows revealed that expansion prevails in the axial flow, and dissipation – in the peripheral flow. The expansion of flow causes the cooling of the axial flow. The mechanical energy is transferred from the axial to peripheral flow by friction and intensifies the dissipation processes which cause an increase in the temperature of the heated part of gas. This interpretation is quite legitimate, because it agrees with the well-known hypothesis of vortex

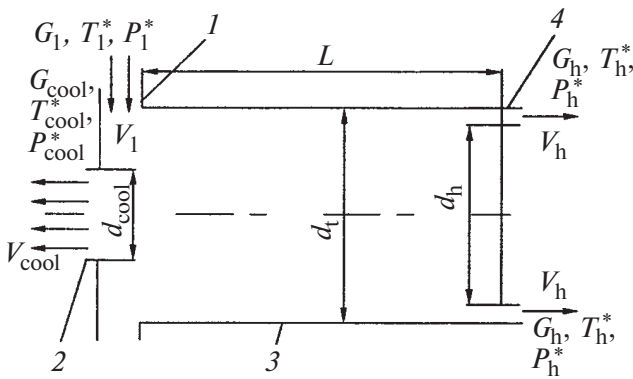


Fig. 1. Design diagram of a return-flow energy separator.

interaction but offers a somewhat different interaction mechanism of its own.

FORMULATION OF THE PROBLEM

It is seldom that one can perform an experimental investigation of swirling flows, because it is very labor-consuming and calls for much time and power. At the same time, the development of computer technologies and the present-day level of numerical calculations, as well as the capabilities of modern personal computers, make it possible to replace full-scale physical experiment by numerical experiment with computerized visualization of flows and obtain interesting data about the physics of relevant processes.

This paper deals with the study of the effect of energy separation known as the vortex or Ranque effect realized in the course of an intense swirling flow in an axisymmetric channel. Limiter elements are installed on the channel end surfaces, i.e., a throttle at the “hot” end and an orifice plate with central opening at the “cold” end. Given a certain combination of the process and design control parameters, the cooled part of initial swirling flow flows from the orifice opening and the heated part of this flow – from the throttle. The physics of redistribution of energy in the vortex tube is a result of complex thermal-and-gasdynamics processes occurring in the energy separation chamber. The simplicity and high reliability of design of the vortex energy separation are regarded as some of its main advantages as a device for the production of cooled masses of gas [1].

The structure of a return-flow Ranque–Hilsch vortex tube is shown in Fig. 1. It consists of a body with a swirling nozzle inlet 1. The body end is usually closed by an orifice plate 2 pressed against the nozzle inlet 1 and provided with a central (in some designs,

adjustable) opening for the removal of masses of initial compressed gas cooled in an energy separation chamber 3. The internal surface of the nozzle inlet which forms a swirling flow is contoured on the Archimedean spiral with the minimal radius equal to that of the energy separation chamber. The throttle device is fashioned as an annular gap on the end wall. Varying the flow area of the gap helped adjust the fraction of cold flow.

NUMERICAL SIMULATION

Solid-state design systems were used to construct three-dimensional models of the vortex energy separator scheme being investigated; these models were used to generate a grid with the aid of the HEXA universal grid plotter [4].

The vortex tube geometry was selected such as to compare the calculation results with those of previous investigation [2]. The tube diameter was $d_t = 94$ mm, the relative length of the energy separation chamber $\bar{l} = L/d_t = 5.5$, the relative radius of the orifice opening $\bar{d}_{cool} = d_{cool}/d_t = 0.36$, and the relative area of the nozzle inlet $f_n = f_n/f_t = 0.05$. The grid was generated in Cartesian coordinates. The grid containing 150 thousand cells was structured, with the points crowding towards the wall. The cell closest to the wall was 0.1 mm in size.

The commercially available CFX-TASKflow code [4] was used to perform numerical simulation and calculation of the velocity and temperature fields in the volume of the energy separation chamber of vortex tubes. In so doing, the mathematical model presumed that the flow is described by a set of three-dimensional Navier–Stokes equations and equations of energy and state. The turbulent viscosity was determined at the initial stage of calculations by the SST model [3] which was later replaced by the $k-\epsilon$ model [3]. This replacement had almost no effect on the pattern and results of calculations. The nonstationary problem was solved by the time relaxation method until steady-state turbulent flow was realized.

The initial mathematical model of description of the processes occurring in the vortex tube consisted of the conservation equations for mass,

$$\frac{\partial \rho}{\partial t} + \frac{\partial}{\partial x_j}(\rho U_j) = 0,$$

momentum,

$$\frac{\partial}{\partial t}(\rho U_i) + \frac{\partial}{\partial x_j}(\rho U_i U_j) = -\frac{\partial P}{\partial x_i} - \frac{\partial \tau_{ij}}{\partial x_j} + \rho f_i,$$

energy,

$$\begin{aligned} \frac{\partial}{\partial t}(\rho H) + \frac{\partial}{\partial x_j}(\rho U_j H) = \\ = \frac{\partial P}{\partial t} - \frac{\partial}{\partial x_j}(U_i \tau_{ij} + Q_j) + \rho U_i f_i \end{aligned}$$

and state,

$$PV = RT.$$

The set was closed using the k - ε model of turbulence [3].

The boundary-value and initial conditions were preassigned in the form of adiabaticity and no-slip conditions. The total pressure $P_1^* = 0.6$ MPa and total temperature $T_1^* = 298$ K were taken to be known at the inlet to the vortex energy separator, and the static pressure – at the outlet. The time step was 10^{-4} to 10^{-5} s.

DISCUSSION OF THE RESULTS

The calculation results confirmed that two vortices rotating in the same direction and moving in opposite axial directions are formed in the energy separation chamber of the vortex tube (Fig. 2a). The formation of these vortices was first observed experimentally by Shults–Grunow [5] and later by other researchers [1]. The energy and gasdynamic interaction of vortices forms the basis of the physical model of description of the process of energy separation. This model is known as the hypothesis of vortex interaction.

The computer visualization (Fig. 2a) leads one to infer that the circumferential component of velocity exceeds appreciably the axial component (see Fig. 2). While the axial component of velocity of peripheral vortex varies insignificantly with increasing distance along the energy separation chamber from the nozzle inlet to the throttle, the decrease in the circumferential component of velocity (attenuation of rotational motion) is more significant, which causes an increase in the pitch of helical lines. This effect is also employed in the hypothesis of vortex interaction. That is why the radial pressure gradient decreases from the nozzle section to the throttle and the static pressure on the axis increases to cause the emergence of the axial

pressure gradient directed from the throttle to the axis of the orifice plate. At the same time, the swirling of axial masses of gas leaving the energy separation chamber via the orifice opening is appreciably lower, which may be attributed to the increase in the axial component of velocity of forced axial vortex in the nozzle cross section of the vortex tube at the outlet from the orifice opening.

Numerical calculation results given in the form of computer visualization confirmed the presence of precessional axial vortex core (Fig. 2b) [1, 6–8] and the formation of large-scale vortex structures arranged periodically along the axis (Fig. 2c) [1, 9], i.e., secondary vortex flows whose rotation occurs in two mutually perpendicular planes. One can assume that the mass transfer by these vortices in the radial direction in the presence of radial pressure gradient makes a contribution to temperature separation in the process of realization of quasi-cooling cycles. Owing to continuous transport of a mass of gas from the axial regions to the peripheral one and back define the transfer of rotational momentum required for swirling the axial vortex from the peripheral to axial vortex.

The behavior of circumferential component of velocity differs from the well-known tangential distribution of Rankine vortex by continuous (without discontinuity) transition on the radius of separation of quasi-solid axial vortex and peripheral potential vortex.

The distributions of circumferential component of velocity (Fig. 3c) agree qualitatively with the experimental data [1, 9]. The quantitative discrepancy may be attributed to differences in the structural elements used in calculations and experiments, as well as to insufficient reliability of experimental data.

Analysis of the distribution of axial velocity (Fig. 3a) confirms the existence of a return flow in the central region of the orifice opening, i.e., of secondary recirculation motion directed into the energy separation chamber. The axial velocity of peripheral heated masses of gas with relative radii $\bar{r}_2 < \bar{r} < 1.0$ almost does not vary along the energy separation chamber (from the nozzle to throttle cross section, $\bar{x} = 5.5$). At the same time, the axial component of axial layers under the effect of the axial pressure gradient increases appreciably from being close to zero in the throttle cross section to $V = 45$ – 50 m/s at the outlet from the orifice opening.

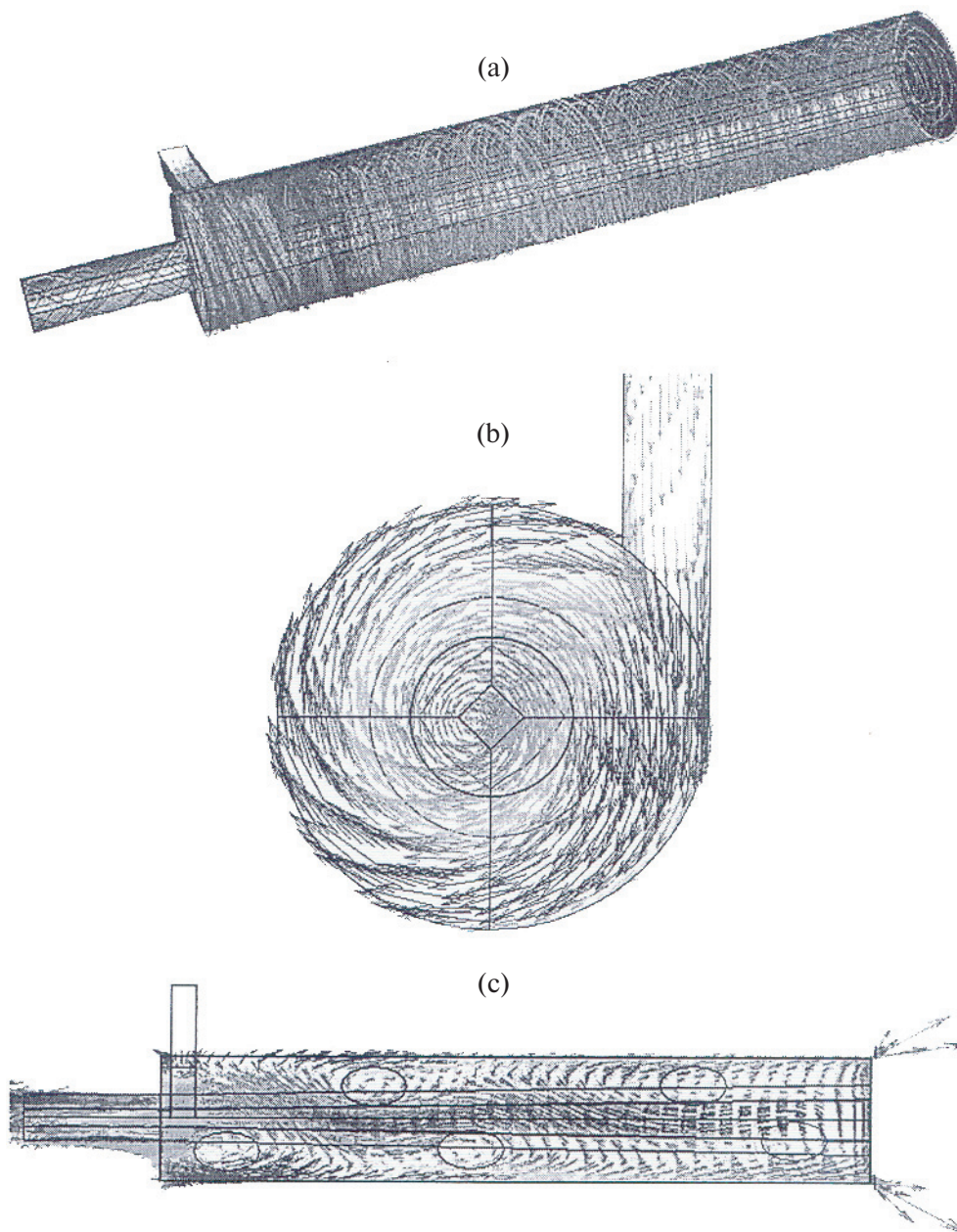


Fig. 2. Computer visualization of flow in a vortex chamber: (a) formation of rotating vortices, (b) precession of vortex core, (c) formation of large-scale vortex structures, secondary flows.

The radial component of velocity increases significantly compared to the other two components only in the extreme cross sections in which interacting vortices are formed, namely, in the nozzle inlet cross sections and in the throttle end cross section. In the remaining cross sections of the energy separation chamber, the radial component of averaged flow does not exceed 2–5 m/s and increases somewhat in the local regions of generation of large-scale vortex structures.

The pattern of distributions of the axial and tangential components of velocity almost does not differ from that obtained experimentally [8]. It does not appear possible to compare the distribution profile of radial component of velocity, obtained by the numerical method, to experimental data. It is rather difficult to experimentally measure the radial component of velocity because of significant radial gradients of thermal-and-gasdynamics parameters, which complicates the process of measurement proper and causes an appreciable decrease in its accuracy. It follows

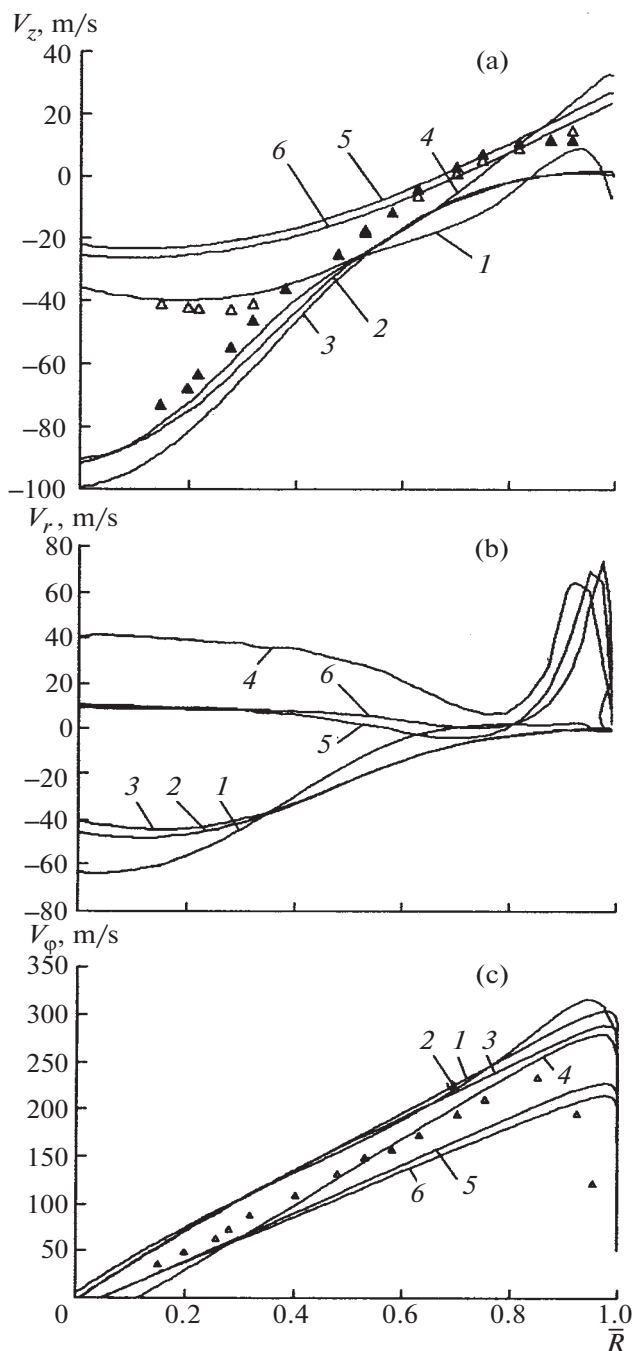


Fig. 3. Velocity profiles: (a) axial component of velocity, (b) radial component of velocity, (c) tangential component of velocity; (1, 2, 3) distributions of velocities in the nozzle cross section $\bar{x} = 0.2$, $\pi = 6$, $\bar{d}_{cool} = 0.37$, $\bar{f}_h = 0.05$, $\bar{I} = 5.5$: (1) $\bar{f}_h = 0.2$, (2) 0.09, (3) 0.04; (4, 5, 6) distribution of velocities over the cross section $\bar{x} = 2.8$, $\pi = 6$, $\bar{d}_{cool} = 0.37$, $\bar{f}_h = 0.05$, $\bar{I} = 5.5$: (4) $\bar{f}_h = 0.2$, (5) 0.09, (6) 0.04; the points indicate the experiment of [8], $\mu = 0.67$, $\pi = 3.77$, $D = 64$ mm, $\bar{d}_{cool} = 0.508$, $\bar{f}_h = 0.09$, $\bar{I} = 9$.

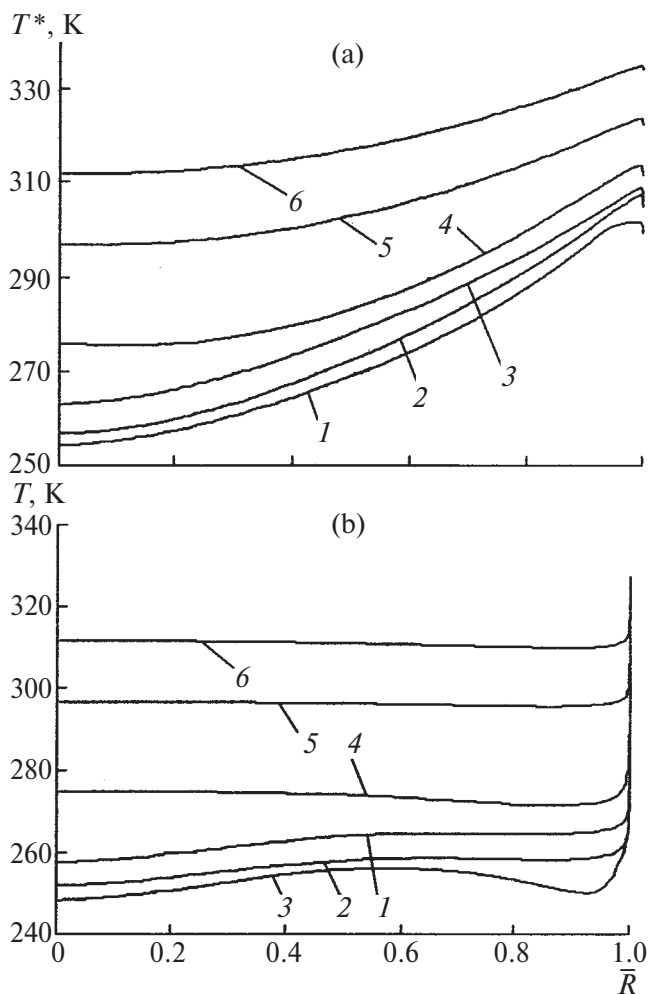


Fig. 4. The distribution of (a) stagnation temperature and (b) static temperature over the vortex tube cross section: (1, 2, 3) nozzle cross section $\bar{x} = 0.2$, $\pi = 6$, $\bar{d}_{cool} = 0.37$, $\bar{f}_h = 0.05$, $\bar{I} = 5.5$: (1) $\bar{f}_h = 0.2$, (2) 0.09, (3) 0.04; (4, 5, 6) cross section $\bar{x} = 2.8$, $\pi = 6$, $\bar{d}_{cool} = 0.37$, $\bar{f}_h = 0.05$, $\bar{I} = 5.5$: (4) $\bar{f}_h = 0.2$, (5) 0.09, (6) 0.04.

from Fig. 3a that a minor deviation of the axial position of sensor may cause a significant variation of its readings (including a change for the opposite) if the measurements are made in the vicinity of dislocation of a large-scale vortex structure.

One can see in Fig. 4a that, as regards the magnitude of the decrease in total temperature, the effects of energy separation agree adequately with the experimental data obtained by Shtym [10] and with the results given in the monograph [1].

The pattern of distribution of static temperature depends largely on the axial position of the cross section in which the measurement is performed. The clos-

er the cross section is to the throttle of the vortex tube, the more uniform the static temperature distribution is (Fig. 4b). This may apparently be attributed to the effects of stagnation of peripheral vortex on the throttle end surface and intensive mixing which provides (as follows from the pattern of variation of the radial component of velocity) for the leveling of static temperature.

CONCLUSIONS

The numerical investigation of flow in the energy separation chamber of a vortex tube resulted in obtaining patterns of flow development, as well as velocity and temperature fields, over the tube volume. It has been demonstrated that two vortices are formed in the chamber, which move in opposite axial directions, namely, a peripheral heated vortex exhibiting a higher than initial enthalpy and an axial vortex whose stagnation enthalpy is much lower. The calculation results confirm the presence of precession of axial quasi-solid core of vortex flow, as well as the generation of large-scale vortex structures of shear pattern which merge into a vortex core moving from the nozzle inlet to throttle. The flow structure in the region of orifice opening is indicative of the generation of secondary flow in the form of recirculating axial vortex.

The results of numerical computer visualization and calculation may be further used for refining the physical model and procedure of calculation of the characteristics of vortex tubes.

NOTATION

d , diameter in the characteristic cross section;
 f , cross-sectional area, m^2 ; H , enthalpy of gas flow,

J/kg ; L , length of the energy separation chamber, m ;
 P , pressure, Pa ; r , radius of the characteristic cross section, m ; R , gas constant, $J/(kg\ K)$; t , time, s ; T , temperature, K ; U , gas flow velocity, m/s ; x , coordinate, m ; V , specific volume, m^3/kg ; μ , relative fraction of flow; $\pi = P_1/P_x$, pressure decrease ratio; ρ , density, kg/m^3 ; τ , shear friction stress.

Subscripts: 1, parameters at the inlet; 2, parameters on the vortex separation radius; h, heated flow; or, orifice plate; ch, energy separation chamber; n, nozzle, cool, cooled flow; t, tube

REFERENCES

1. Piralishvili, Sh.A., Polyayev, V.M., and Sergeev, M.N., *Vikhrevoi effect. Eksperiment, teoriya, tekhnicheskie resheniya* (Vortex Effect: Experiment, Theory, Technical Solutions), Leontiev, A.I., Ed., Moscow: UNPTs Energomash, 2000.
2. Frohlingdorf, W. and Unger, H., *Int. J. Heat Mass Transfer*, 1999, no. 42, p. 415.
3. *CFX-TASKflow Theory Documentation Version 2.12*, AEA Technology Engineering Software Limited, Waterloo, Ontario, Canada, N2L5Z4.
4. *CFX-TASKflow User Documentation Version 2.12*, AEA Technology Engineering Software Limited, Waterloo, Ontario, Canada, N2L5Z4.
5. Shults-Grunow, F., *Kaltetechnik*, 1950, vol. 2, p. 273.
6. Arbuzov, V.A., Dubnischchev, Yu.N., Lebedev, A.V., *et al.*, *Zh. Tekh. Fiz.*, 1997, vol. 23, no. 23, p. 84.
7. Knysh, Yu.A., *Inzh. Fiz. Zh.*, 1982, vol. 37, no. 1, p. 59.
8. Alekseenko, S.V. and Okulov, V.L., *Teplofiz. Aeromekh.*, 1996, vol. 3, no. 2, p. 101.
9. Lukachev, S.V., *Inzh. Fiz. Zh.*, 1981, vol. 41, no. 5, p. 784.
10. Shtym, A.N., *Aerodinamika tsiklonno-vikhrevykh kamer* (Aerodynamics of Cyclone Chambers), Vladivostok: Dal'nevostochnyi tekhnicheskii institut (Far-Eastern Technical Inst.), 1984.